AN INSIDE VIEW OF PSEUDORANGE AND DELTA PSEUDORANGE MEASUREMENTS IN A DIGITAL NAVSTAR GPS RECEIVER

Phil Ward (214) 462-4910
Senior Member of the Technical Staff
Texas Instruments Incorporated
P.O. Box 405, M.S. 3418
Lewisville, Texas 75067

ABSTRACT

The goal of this paper is to develop insight into the real-time nature of GPS observables measured by a digital receiver. The concept of how independent pseudorange and delta-pseudorange measurements are captured as a by-product of the code and carrier tracking loops of a digital NAVSTAR GPS receiver is explained. The classical equations defining true range and delta range are derived in terms of pseudorange and delta pseudorange. The actual GPS receiver measurements are then related to these equations. The difference between GPS measurement resolution and precision is treated and the sources of the GPS receiver contribution to the total GPS error are identified. The total GPS error, in terms of user equivalent range error (UERE) and user equivalent delta range error (UEDRE), is characterized. However, an unaided GPS navigation process can filter out only the unbiased random error in the observables, not the total UERE and UEDRE content. Also, the random error in GPS observables is not stationary. Hence, the random error in UERE and UEDRE is identified and characterized.

INTRODUCTION

Advantages in using digital techniques to design a NAVSTAR GPS receiver are numerous, Many of these advantages have been described in references 1 and 2. This paper describes the advantage of direct measurements of pseudorange and delta pseudorange in a digital receiver. A digital receiver is a receiver whose code and carrier-loop frequency synthesizers use numerically controlled or digital oscillators (DOs). The frequency output of a DO is determined by a digital number applied to its input. A block diagram of a typical digital GPS receiver is shown in Figure 1. An analog receiver is a receiver with code and carrier loop frequency synthesizers that use voltage-controlled crystal oscillators (VCXOs). The frequency output of a VCXO is determined by an analog voltage applied to its input. A block diagram of a typical analog GPS receiver is shown in Figure 2. The

important distinction between the DO of the digital receiver and the VCXO of the analog receiver is that the instantaneous analog phase state of a VCXO can be neither controlled nor measured directly, whereas the discrete phase state of a DO can be controlled and measured directly.

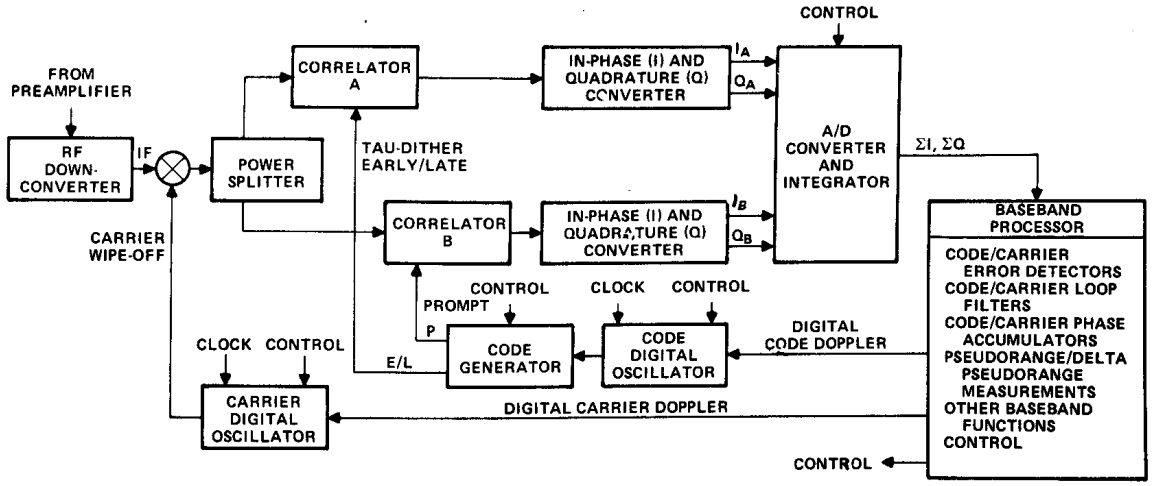

Figure 1 - Typical Digital Receiver Block Diagram.

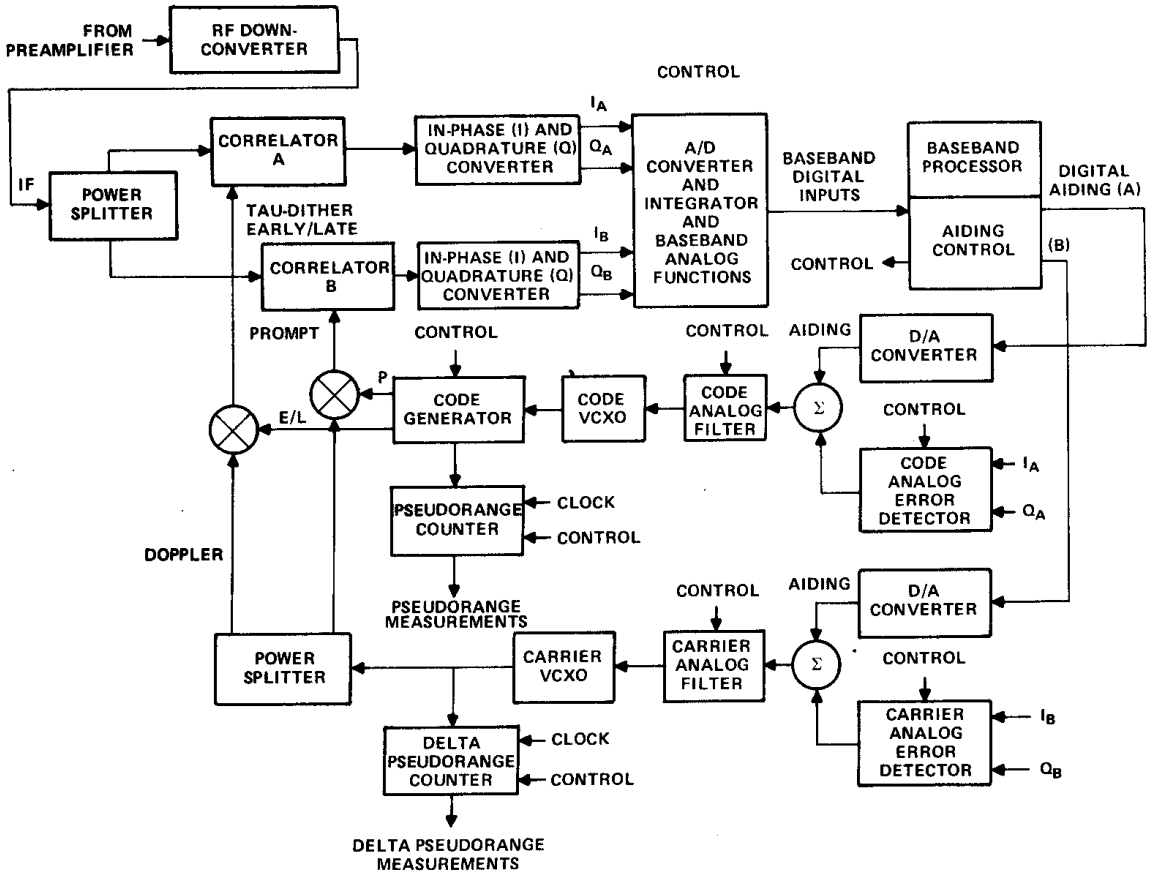

Figure 2-Typical Analog Receiver Block Diagram.

GPS Observables

The chief role of a GPS receiver front end is to measure pseudorange and delta pseudorange with respect to at least four GPS space vehicles (SVs) and to read the 50-Hz signal (navigation message) data from each SV. Pseudorange can be derived directly and precisely from the instantaneous discrete replica code phase state in the code loop of a digital receiver. Delta pseudorange can be derived directly and precisely from the measurement of the instantaneous discrete replica carrier phase state in the carrier loop of a digital receiver. The 50-Hz signal data can be read only when the receiver is in phase lock with the SV carrier. When in phase lock, the 50-Hz signal data are read as a direct by-product of the integrated in-phase component of the digitized carrier loop baseband input signal. The carrier loop in-phase (I_p) and quadrature (Q_P) signals are usually derived from a prompt (or on-time) code-correlation narrowband channel. In Figures 1 and 2, where the receiver block diagrams are shown in closed-loop operation (rather than search operation), I_B and Q_B in the figures correspond to I_p and Q_p, respectively.

DEFINITION OF TRUE GPS RANGE

Suppose a GPS space vehicle (SV) transmitted a particular code epoch at T_t, GPS transmit time and the GPS user receiver was correlated perfectly with this code epoch at T_r GPS receive time. If no other propagation delays between SV(j) and user-antenna phase center need be considered, the ideal true range $\hat{R}(j)$ would be given by $\hat{R}(j) = c \cdot [T_r(j) - T_t(j)]$ meters, where c is the GPS value for speed of light (2.99792458×10^8 m/s, $T_r(j)$ and $T_t(j)$ are in seconds, and the index indicates the jth SV. However, the GPS signal has several delays which, if not subtracted, would make the range measurement of this equation longer than the true range. These delays include the frequency-independent tropospheric delay (TD_t) and frequency-dependent ionospheric delay (TD_i), which are the combined atmospheric delay (TD_a) effect. Also, there are receiver delays (TD_r) between the antenna phase center and the code-correlation point in the receiver. Taking these delays into account, the equation becomes $R(j) = c \cdot [T_r(j) - T_t(j) - TD_a(j) - TD_r(n)]$ meters where R(j) = true range, $TDa(j) = TD_i(j) + TD_t(j)$ in seconds, and the index n in $TD_r(n)$ refers to the receiver channel. Figure 3 shows this GPS time relationship.

The essential reason for two frequencies (the primary frequency at L_1 = 1575.42 MHz and the secondary frequency at L_2 = 1227.60 MHz) from each SV is to measure ionospheric delay. This is done in a two-frequency receiver by measuring the range difference to SV(j) between the two frequencies and then multiplying the difference by a scale factor K_i given by $K_i = 1/[1 - (L_1/L^2)^2] = -1.546$. The ionosphere has a delay effect that is approximately inversely proportional to the square of the frequency. Single-frequency receivers must model the ionospheric correction, unless it is provided by another means external to the receiver. The tropospheric correction must be modeled in either case, because tropospheric

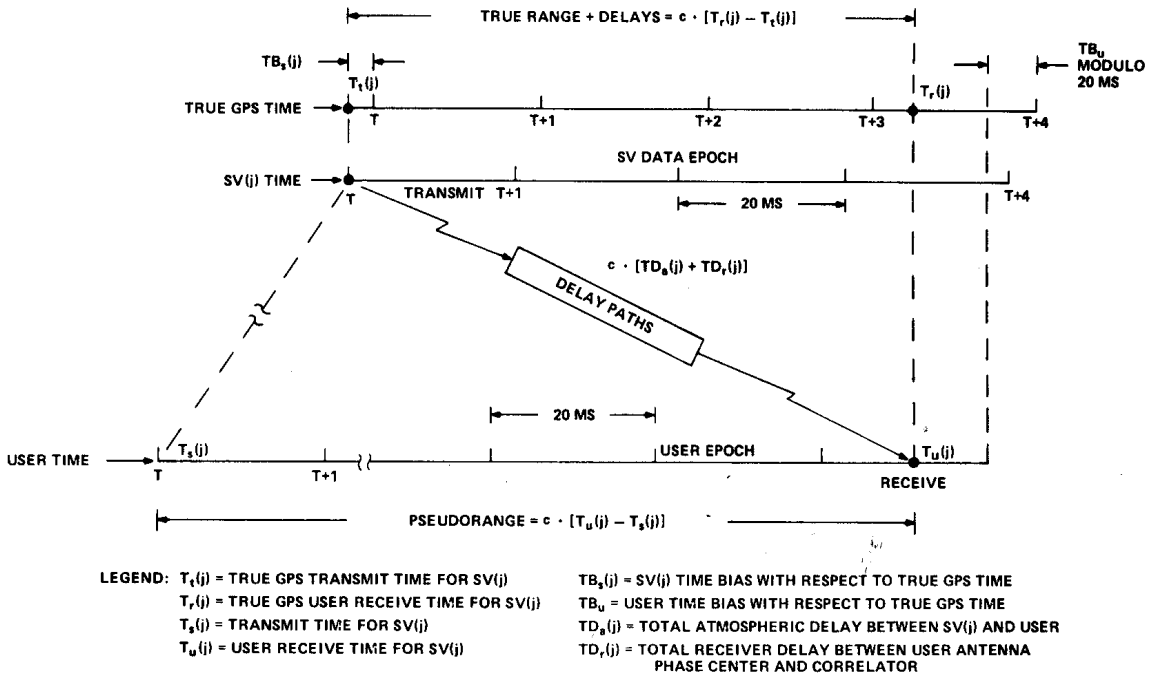

Figure 3 - GPS Transmit and Receive Time Relationships.

delays are independent of frequency. One example of a model for this correction is given by the following formula: $TD_t(j) = [c_1 / \sin(\alpha_j)] \cdot e^{-c2 \cdot h}$ seconds where c_i is a constant: 7.365×10^{-9} ; c_2 is a constant: 1/6,900; α_j is the elevation angle above horizontal from user to SV(j); and h is the altitude of the user above the earth's surface (meters). It has been estimated that the combined effect of modeling TD_a results in a range error of from 2.44 to 5.18 meters (reference 3).

In general, the GPS SVs are not perfectly aligned with respect to true GPS time and their clocks drift slightly with respect to true GPS time. However, their time offset and drift characteristics are precisely measured by the control segment and transmitted as three polynomial coefficients a_0, a_1, and a_2 in the clock-correction portion of the SV navigation message data. Thus, the range equation is further modified to include the SV(j) transmit time bias offset $TB_s(j)$ with respect to true GPS time, so that $R(j) = c \cdot [T_r(j) - T_s(j) + TB_s(j) - TD_a(j) - TD_a(n)]$ meters, where $T_t(j) = T_s(j) - TB_s(j)$ and $T_s(j)$ is the SV(j) transmit time according to its own clock, which, when corrected by the offset time $TB_s(j)$, equals true GPS transmit time, $T_t(j)$. The clock correction is determined as follows: $TB_s(j) = a_0 + a_2 [T_s(j) - t_{oc}(j)] + a_2 [T_s(j) - t_{oc}(j)]^2$, where a_0, a_1, and a_2 are polynomial coefficients and $t_{oc}(j)$ is the GPS reference time obtained from the SV(j) navigation message data. Negligible accuracy is lost if $T_s(j)$ is replaced with user receive time T_u.

The user receiver clock, with respect to true GPS time, is misaligned and drifts. Therefore, the user must determine the offset or time bias TB_u with respect to true GPS time by incorporating one more SV(j) measurement than is required to determine position. For

three-dimensional independent position measurement with GPS, four SV measurements are used, so that four nonlinear equations can be formulated to solve four unknowns: x_u, y_u, z_u, (user position) and TB_u (user time bias). Finally, the range equation is modified to reflect the user time bias with respect to true GPS time:

$$R(j) = c \cdot [T_u(j) - T_s(j) + TB_s(j) - TD_a(j) - TD_r(n) - TB_u] \text{ meters} \quad (1)$$

where $T_r(j) = T_u(j) - TB_u$, and TB_u is not indexed since it will be the same user time bias for all measurements at the same user receive time T_u.

DEFINITION OF PSEUDORANGE

Equation (1) reflects the measurements that a GPS receiver uses to determine true range to SV(j). The definition of pseudorange is in terms of the raw receiver measurements before applying delay corrections and before having determined time bias. Pseudorange is defined as:

$$PR(j) = c \cdot [T_u(j) - T_s(j)] \text{ meters} \quad (2)$$

This can be thought of as the measurement of the apparent range to SV(j), using the transmit time $T_s(j)$ that SV(j) thinks is true GPS time and the receive time $T_u(j)$ that the user estimates is true GPS time (reference 4). Both times have time-bias corrections that must be applied and the result must be corrected for delay paths encountered to arrive at true range. Equation (1) can be written in terms of pseudorange from equation (2) as follows:

$$R(j) = PR(j) + c \cdot [TB_s(j) - TD_a(j) - TD_r(n) - TB_u] \text{ meters} \quad (3)$$

However, a digital GPS receiver does not measure pseudorange directly. What it does measure directly in the code-tracking loop is replica code phase which is effectively the satellite transmit time $T_s(j)$. The replica code phase state for a P-code receiver is measured in P-chips, $\phi_{co}(j)$. In this case, equation (2) is changed as follows:

$$PR(j) = c \circ [T_u(j) - \phi_{co}(j)/f_o] \text{ meters} \quad (4)$$

where $\phi_{co}(j)$ is the number of P-code chips and fractions of a chip that have elapsed since the GPS beginning of the week corresponding to SV(j) transmit time; and f_o is the code chipping rate (10.23×10^6 chips/sec for P-cocle). Thus, $\phi_{co}(j) \equiv T_s(j) \cdot f_o$ chips. If $\phi_{co}(j)$ is in C/A-chips, f_o is 1.023×10^6. For C/A-only operation, the SV(j) transmit time rolls over every 1,023 C/A chips or every 1 millisecond. Special care must be taken in Equation

(4) to correct for end-of-week and (if applicable) C/A chip rollover effects when they occur.

For the two-frequency user the code phase is measured in both L_1 (ϕ_{co1}) and L_2 (ϕ_{co2}) resulting in an L_1 pseudrange PR_{L1} and an L_2 pseudorange PR_{L2}. The ionospheric correction is determined using the scale factor previously shown as follows: TD_i (j) = $K_i / f_o \cdot [\phi_{co2}$ (j) - ϕ_{co1} (j)] = K_i [PR_{L1} (j) - PR_{L2} (j)] . For the single-frequency user, both components of TD_a (j) must be modeled and the value for TB_s (j) in Equations (1) or (3) must be corrected for the interchannel bias difference between L_1 and L_2 in SV(j) using T_{GD} (j) in the satellite-clock-correction data.

ANALOGY BETWEEN TRANSMIT TIME AND REPLICA CODE STATE

To track a GPS SV, both the code and carrier state must be replicated in the receiver tracking loops and correlated with the incoming SV signal. If there is zero error between the replicated signals and the incoming SV(j) signal (maximum correlation), the replicated code phase state is linearly analogous to the earlier SV transmit time at the later selected user time event, while the replicated carrier-phase state corresponds to the SV transmit carrier phase. From these raw measurements, usual GPS receiver pseudoranges, delta pseudoranges, and their L_1/L_2 differences can be derived. A number of complex indirect hardware counter schemes exist for extracting these measurements from a GPS receiver; the most straightforward and accurate is to synthesize the code and carrier loops, using numerically controlled (digital) oscillators and digital loop filters so that the measurements of these tracking-phase states become exact by-products of the loop frequency-synthesis process.

ADVANTAGES OF NUMERICALLY CONTROLLED (DIGITAL) OSCILLATOR

The distinct GPS advantages of a DO code synthesizer are: (a) the code phase is precisely measurable because it is advanced in discrete clock increments and (b) the phase increments are derived from one user clock source, the receiver oscillator.

The general advantages of a DO synthesizer for either code or carrier loops are that they are readily applicable to programmable microprocessor-based systems. The DOs are inherently reproducible: there are no potentiometers, no tuning, and no drift or stability problems. Their design is straightforward and they are more versatile than are their analog equivalents. Because they are digital, their design is compatible with the trend toward large-scale integrated (LSI) custom component design. A DO can be defined as a device which produces discrete quantized samples of a waveform at a fixed sample rate. Figure 4 is a block diagram of a basic DO. Figure 5 shows the fundamentals of DO operation.

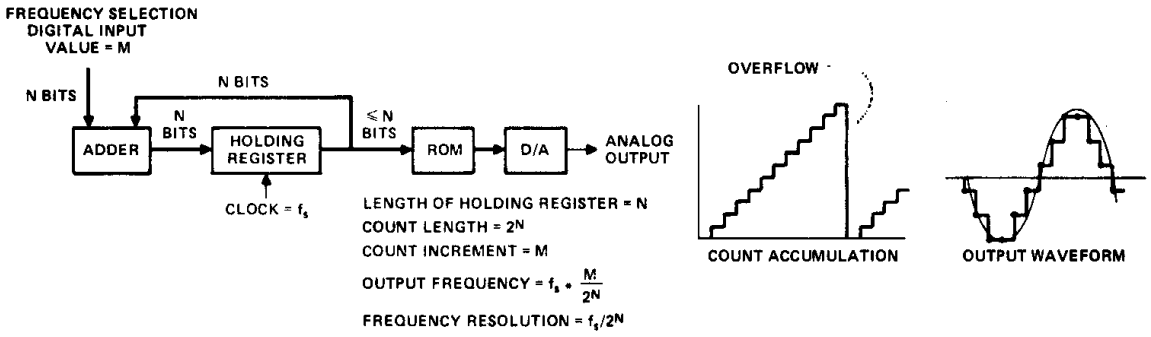

Figure 4 - Digital Oscillator Block Diagram.

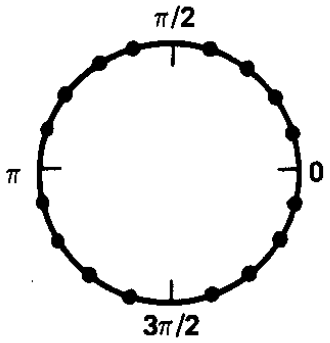

1. PHASE PLANE OF 360° IS SUBDIVIDED INTO M INCREMENTS

2. THESE M POINTS ARE STORED IN READ-ONLY MEMORY (ROM):

   VALUE STORED IN ROM FOR EACH PHASE POINT REPRESENTS AMPLITUDE OF WAVEFORM TO BE GENERATED AT THAT PHASE POINT.

   RATE AT WHICH PHASE PLANE IS TRAVERSED DETERMINES FREQUENCY OF OUTPUT WAVEFORM.

   UPPER BOUND ON AMPLITUDE ERROR IS: $e_{MAX} = 2\pi/M$

   THE APPROXIMATE AMPLITUDE ERROR IS: $e \cong 2\pi/M \cos \phi(t)$ WHERE $\phi(t)$ IS THE PHASE ANGLE

Figure 5 - Digital Oscillator Implementation Concept.

DIGITAL SYNTHESIS OF REPLICA CODE STATE

Figure 6 is a detailed block diagram of a DO design used for a GPS code synthesizer. When tracking in P-code, the replica code generator is advanced at the P-code chipping rate of 10.23 MHz plus doppler. In C/A-code, the C/A-code chipping rate of 1.023 MHz plus doppler is applied. The replica code state is composed of an integer part and a fractional part. To synthesize replica code state in a digital receiver, the integer part of the code state is set into the code generator and the code generator is advanced with the code DO at the code chipping rate plus doppler. At the completion of each cycle of the DO, a carry output advances the code state by one chip. The fractional part of the replica code state at any given user clock event is simply the phase of the code DO at the same user clock event. Its operation is described in more detail in reference 1.

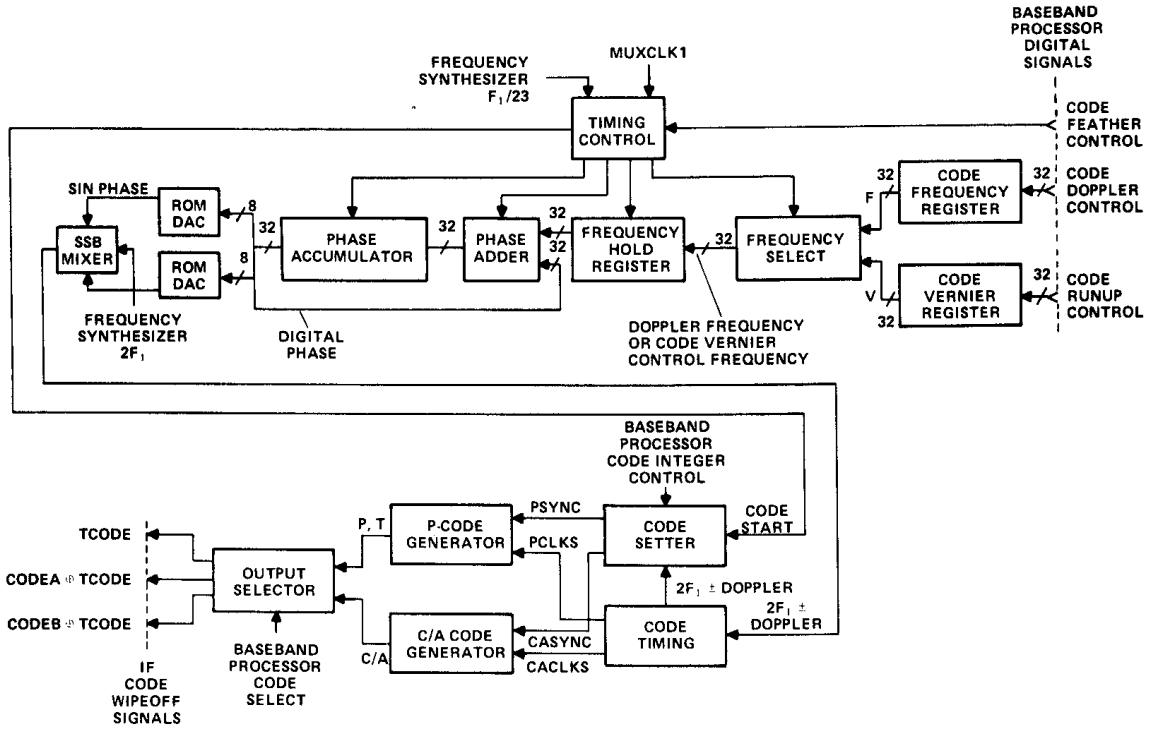

Figure 6 - Code Synthesizer Block Diagram.

DEFINITION OF DELTA RANGE

The change over a specified time interval, in true range to an SV, is called delta range. Delta range divided by the specified time interval is the mean relative velocity between the user and SV(j) for that time interval. Delta range is given by DR(j) = R_2 (j) - R_1 (j) where R2 (j) is the true range at the end of the specified time interval and R_1 (j) is the true range at the start, and by DR(j) = DPR(j) + c · [DTB_s (j) - DTD_a (j) - DTD_r (n) - DTB_u], where DPR = PR_2 - PR_1 , the pseudorange change or delta pseudorange over the interval; DTB_s = TB_{s2} - TB_{s1}, the satellite clock bias change or delta time bias of SV(j) over the time interval; DTD_a = TD_{a2} - TD_{a1}, the atmospheric delay change or delta time delay of atmosphere over the time interval; DTD_r = TD_{r2} - TD_{r1}, the receiver delay change or delta time delay of receiver over the time interval; and DTB_u = TB_{u2} - TB_{u1}, the user clock bias change or delta time bias of user over the time interval. Usually, the atmospheric delay change and the receiver delay change are assumed to be zero and effectively absorbed into the user clock bias change. Hence, the second equation becomes:

$$DR(j) = DPR(j) + c \cdot [DTB_s - DTB_u] \quad (5)$$

The term DTB_u is determined by the navigation solution, and the satellite clock bias change is determined by:

$$DTB_s \cong {}_{a1} \cdot \Delta T + a_2 \cdot (\Delta T)^2 \quad (6)$$

where ΔT is the specified delta range time interval.

The change in pseudorange is measured most easily by reading carrier phase at both start and stop time events of the desired delta pseudorange. Thus, delta pseudorange is given by:

$$DPR(j) = \left(\frac{c}{f_L}\right) \cdot [\phi_{CA2}(j) - \phi_{CA1}(j)] \text{ meters} \quad (7)$$

where ϕ_{ca} = instantaneous user replica carrier phase in cycles at L-band; and f_L = 1575.42 X 10^6 cycles/second for L_1 carrier and 1227.6 X 10^6 cycles/second for L_2 carrier.

DEFINITION OF DELTA PSEUDORANGE

Equation (7) defines delta pseudorange as the change in user replica carrier phase between two user time events times a scale factor. The total carrier phase change must be accounted for between this time interval; hence, integer carrier cycles must be counted as well as the fractional change in phase.

DIGITAL SYNTHESIS OF REPLICA CARRIER PHASE

Figure 7 is a detailed block diagram of a DO design used for a GPS carrier synthesizer. Its operation is described in reference 1.

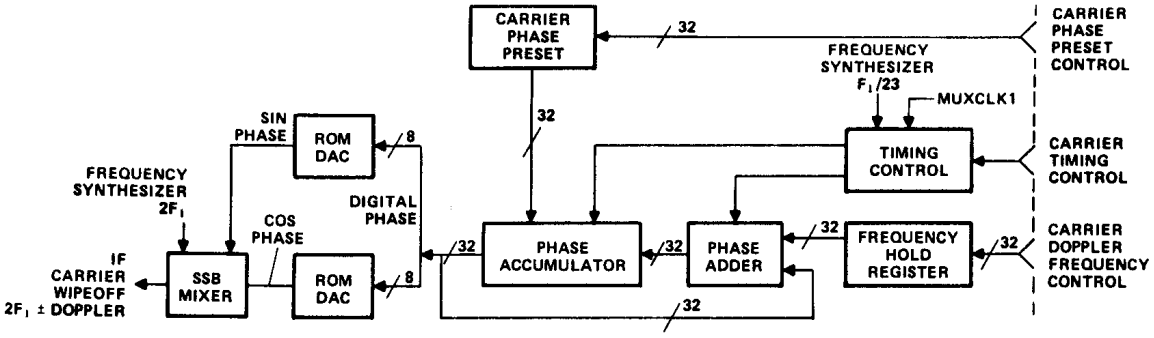

Figure 7 - Carrier Synthesizer Block Diagram.

GPS MEASUREMENT ACCURACY

Table I compares typical analog and digital receiver measurement resolutions. The measurement resolution of a digital GPS receiver is orders of magnitude greater than that of an analog receiver. Hence, measurement error can usually be neglected in a digital receiver, but must always be considered in an analog design. However, measurement resolution is only one of many error contributions to user equivalent range error (UERE) and user equivalent delta range error (UEDRE). The user position error is determined by multiplying position dilution of precision (PDOP) times UERE (reference 3). A similar

relationship is true foruservelocity error and UEDRE. A PDOP of 3 or lesscan be expected in the full GPS 18-SV constellation.

Table II is a typical GPS system pseudorange error budget, including sources of the errors and the nature (statistics) of the errors. Note that the GPS receiver design can only improve on the receiver noise and resolution; the ionospheric delay compensation and, possibly, the antenna design could improve on multipath rejection. Table III is a typical delta pseudorange error budget. Table IV summarizes the components of the receiver code noise and resolution error budget in Table I I for a typical digital receiver.

TABLE 1. Typical Measurement Resolution Comparison

Parameter	Analog Receiver LSB	Digital Receiver LSB
Pseudorange (meters)	1.8 to 9.0	0.0005
Delta pseudorange (meters)	0.003 to 0.015	0.000003

TABLE II. Typical GPS Pseudorange Error Budget

Error Contributor	Error Source[1]	Error Statistics	1-Sigma Error (Meters)
Clock and navigation subsystem stability	SS and CS	Bias	2.7
Predictability of SV perturbations	SS and CS	Bias	1.0
Other	SS and CS	White noise	0.5
Ephemeris and clock prediction	CS	Bias	2.5
Other	CS	White noise	0.5
Ionospheric delay[2] compensation	US	Markov	2.3
Tropospheric delay compensation	US	Bias	2.0
Receiver noise[3] and resolution	US	Markov	1.5
Multipath	US	White noise	1.0
Other	US	White noise	0.5
Total 1-sigma user equivalent range error			5.3

Notes: 1. SS = Space Segment, CS Control Segment, US = User Segment.
2. Ionospheric delay compensation error is related to receiver noise and resolution error by a factor of 1 .546.
3. Receiver noise and resolution error are predictable as functions of several measurable receiver parameters. With all else equal, these errors decrease when C/No increases. The errors shown are the maximum allowable 1-sigma errors for the receiver operating in P-code.

TABLE III. Typical GPS Delta Pseudorange Error Budget

Error Contributor	Error Source[1]	Error Statistics	1-Sigma Error (Meters)
Satellite clock noise	SS	White noise	0.003
Propagation gradient	US	Markov	0.008
Receiver noise[2] and resolution	US	White noise	0.008
Other	US	White noise	0.003
Total 1-sigma user equivalent delta range error[3]			0.012

Notes: 1. SS = Space Segment, US = User Segment.
2. Receiver noise and resolution error are predictable as functions of several measurable receiver parameters. With all else equal, this error decreases when C/No increases. The error shown is the maximum allowable 1-sigma error for the receiver operating in P- or C/A-code.
3. To convert to degrees at L_1, multiply by 1.892×10^3; at L_2, multiply by 1.474×10^3.

Note that thermal tracking jitter is the dominant error source in the code tracking loop. This error can be predicted accurately in real time (reference 5) if an accurate measure of C/No is made in the receiver and the bandwidths of the receiver are provided.

Table V summarizes the components of the receiver carrier noise and resolution error budget in Table III for a typical digital receiver. Thermal tracking jitter variance in a phase-locked carrier loop changes with C/No and can be predicted by:

$$\sigma_{CA}^2 = \frac{B_n}{C/No}\left[1 + \frac{0.5}{(C/No \cdot 1/B_p)}\right] \text{ (radians)}^2 \qquad (8)$$

where B_n is the carrier loop noise bandwidth (Hz), B_p is the predetection bandwidth (Hz), and C/No is the effective signal power to noise spectral density ratio (Hz).

Since the GPS navigation process cannot remove or improve on errors that are “bias-like” over its estimation interval, only the unbiased random error (white noise) components in the observables, rather than the total UERE and UEDRE, content should be considered. The random error in GPS observables is not stationary as a result of changing C/No and sometimes as a result of changing bandwidth and loop-tracking conditions during loop closure or weak signal hold on. If the navigation process comprehends these tracking conditions, the effective total error variance in the code and carrier loops can be predicted in real time. Figures 8 and 9 are typical digital-receiver error plots for pseudorange and delta pseudorange observations from a real SV.

TABLE IV. Typical Digital Receiver Code Loop Tracking Error Budget (P-Code)

Error Contributor	Error Statistics	1-Sigma Error (Meters)
Oscillator stability[1]	Markov	0.30
Code hardware resolution	White noise	Negligible
Code software resolution	White noise	Negligible
Internal multipath	White noise	0.12
RF group delay variation	Markov	0.06
Thermal tracking jitter[2]	Markov	1.45
Other	White noise	0.12
	Total 1-sigma receiver noise and resolution pseudorange error	1.5

Notes: 1. Oscillator stability error increases under acceleration stress. However, this has a small order effect on the code loop error budget.

2. Thermal tracking jitter error is the dominant code loop error source which decreases when C/No increases. The error shown is the maximum allowable 1-sigma error for the P-code receiver design and minimum C/No. For C/A-code operation, multiply P-code thermal tracking jitter error by 10.

TABLE V. Typical Digital Receiver Carrier Loop Tracking Error Budget

Error Contributor	Error Statistics	1-Sigma Error (Meters)
Oscillator stability[1]	Markov	0.003
Carrier hardware phase jitter	White noise	0.001
Carrier software phase jitter	White noise	0.0001
L-Band synthesizer phase jitter	White noise	0.003
Thermal tracking[2] jitter	Markov	0.007
Other	White noise	0.001
	Total 1-sigma receiver noise and resolution	0.008

Notes: 1. Oscillator stability error increases under acceleration stress. This can have a significant effect on the carrier loop error budget. The error shown is the maximum allowable 1-sigma error under maximum specified acceleration stress.

2. Thermal tracking jitter error may not be the dominant carrier error source. This error decreases when C/No increases. The error shown is the maximum allowable 1-sigma error for the receiver design and minimum C/No when operating in P- or C/A-cocle.

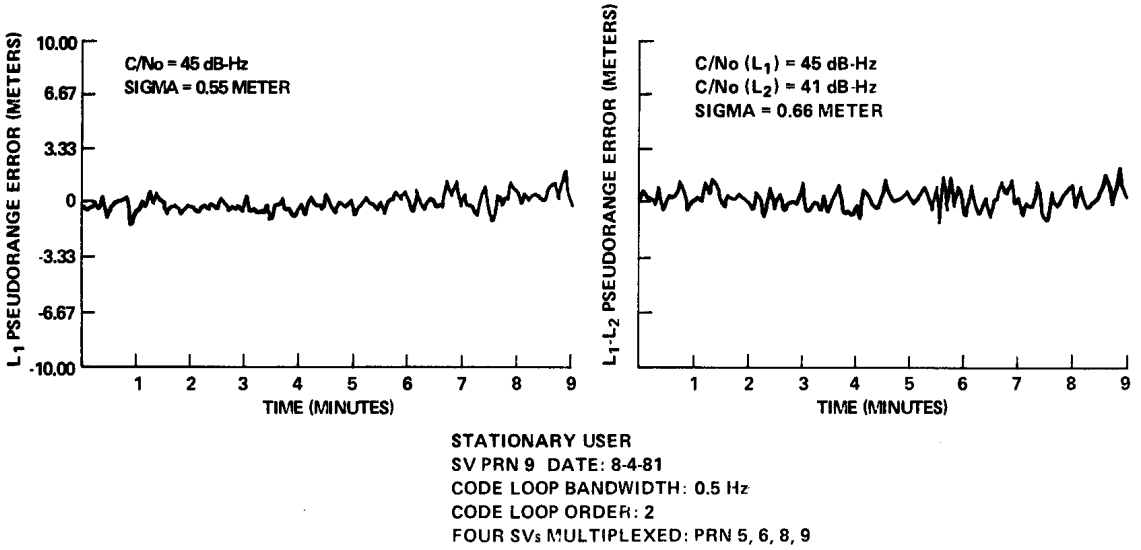

Figure 8 - L_1 and L_1-L_2 Pseudorange Error Plots

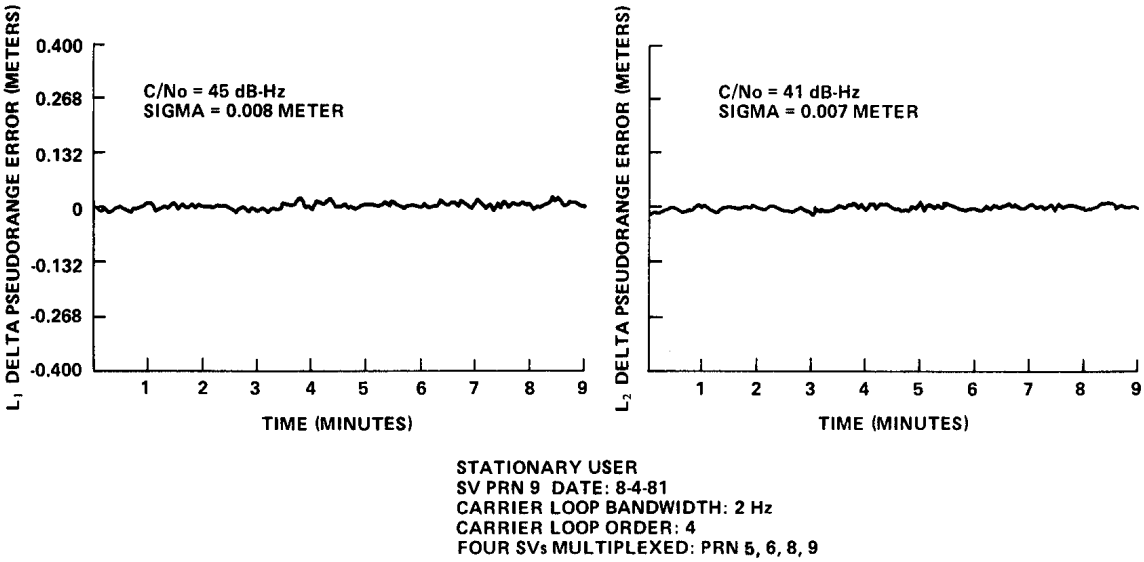

Figure 9 - L_1 and L_1-L_2 Delta Pseudorange Error Plots

SUMMARY

The real-time nature of GPS observables, as measured by a digital receiver, has been described, starting with the classical equations that define true range and delta range in terms of pseudorange and delta pseudorange. The concept of how pseudorange and delta pseudorange measurements are captured as a by-product of the digital oscillator phase states in the code and carrier tracking loops of a digital receiver has been described. The advantages of digital oscillators over their analog counterparts were summarized. The difference between measurement resolution and accuracy was discussed. The total GPS error sources were identified in terms of user-equivalent range error (UERE) and user equivalent delta range error (UEDRE). The unbiased random error (white noise) components were identified since these are the only components that an unaided GPS navigation process can recognize and filter. The white noise components that change with C/No were also identified and a way to predict these in real time was described.

REFERENCES

1. Ward, P.W. (1980). “An Advanced NAVSTAR GPS Multiplex Receiver,” IEEE PLANS ’80.

2. Johnson, C.R., et al (1981). “Applications of a Multiplexed GPS User Set,” Institute of Navigation National Meeting.

3. Milliken, R.J. and Zoller, C.J. (1978). “Principle of Operation of NAVSTAR and System Characteristics,” Journal of the Institute of Navigation, Vol. 25, No. 2.

4. Van Dierendonck, A.J., et al (1978). “The GPS Navigation Message,” *Journal of the Institute of Navigation*, Vol. 25, No. 2.

5. Hartman, H.P. (1974). “Analysis of a Dithering Loop for PN Code Tracking,” *IEEE Transactions on Aerospace and Electronic Systems*, Vol. AES-10, No. 1.